



## Clean demarcation of cartilage tissue $^{23}\text{Na}$ by inversion recovery

Peng Rong, Ravinder R. Regatte, Alexej Jerschow\*

Chemistry Department, New York University, 100 Washington Square East, Room 966, New York, NY 10003-6621, USA  
Radiology Department, Langone Medical Center, New York University, New York, NY 10003, USA

### ARTICLE INFO

#### Article history:

Received 14 December 2007

Revised 25 April 2008

Available online 1 May 2008

#### Keywords:

Inversion recovery

Sodium-MRI

Ordered sodium

Free sodium

Cartilage imaging

### ABSTRACT

Monitoring the sodium concentration in vivo using  $^{23}\text{Na}$  MRI can be an important tool for assessing the onset of tissue disorders. Practical clinical  $^{23}\text{Na}$  MRI methods furthermore often do not allow one to use sufficiently small voxel sizes such that only the tissue of interest is seen, but a large signal contamination can arise from sodium in synovial fluid. Here we demonstrate that applying an inversion recovery (IR) technique allows one to distinctly select either the cartilage-bound or the free sodium for visualization in an image. The results are validated both ex vivo and in vivo.

© 2008 Elsevier Inc. All rights reserved.

### 1. Introduction

A large amount of sodium exists in living tissues, such as cartilage and the brain, which makes  $^{23}\text{Na}$  MRI a very promising tool for the diagnosis of cartilage pathologies, as well as, brain tumors [1]. Notably, the cartilage tissue sodium concentration has been shown to correlate directly with the decrease of the proteoglycan content, which is frequently identified with the onset of degenerative joint disease [2–8].

Normally, the signals from free sodium and the cartilage-bound or ordered sodium overlap with each other, and several methods have been developed for their separation. A number of techniques are based on the evolution under residual quadrupolar interactions. For example, in the double-quantum filter experiment [9,10], the transverse magnetization operators  $T_{\pm 1}^1$  evolve into second rank tensors under the action of the quadrupolar interaction. These second-rank tensors can then be converted into double-quantum coherences ( $T_{\pm 2}^2$ , which can be filtered out using phase cycling). Alternatively, in the Jeener–Broecker experiment the rotational properties of different rank tensors [9] are exploited to perform this selection. Both techniques were adapted to detect the filtered signal through the central transition to obtain higher signal-to-noise ratio and higher resolution [9], however they require a large phase cycle and are difficult to implement on MRI scanners since they use a large number of pulses. More recently, methods based on frequency-sweep pulses [11,12] and quadrupolar nutation [13] were demonstrated, which exploit coherence transfer properties that depend on the quadrupolar interaction.

The quadrupolar coupling itself was shown to correlate with the onset of cartilage degeneration [14,15].

Another form of signal separation is performed by the triple quantum filtered experiments, in which the selected signal arises from quadrupolar nuclei in slow motion [16]. Slow-motion gives rise to third-rank tensors, which, upon conversion to triple-quantum coherences, can be filtered out by phase cycling.

In the current study, we demonstrate the feasibility of employing the inversion recovery (IR) sequence to selectively detect the cartilage-bound sodium signal or the free sodium signal. The study shown here depends on the significant difference between the spin–lattice relaxation rates between the two pools. In the particular case of cartilage tissue, the difference is especially large due to immobilization and larger induced quadrupolar interactions of the bound sodium. It is possible that cartilage-tissue also contains free sodium, as one could expect in analogy to experiments performed with  $^2\text{H}$  [17,18], but we have not seen a significant fraction thereof in bulk measurements [15]. Sodium inversion recovery has been used in brain imaging [20] and in mouse tumor imaging [21].

A large fraction of the signal is typically lost in  $^{23}\text{Na}$  MRI due to lengthy rf-pulses. The simplicity of the inversion recovery sequence makes it hence particularly attractive for  $^{23}\text{Na}$  MRI.

### 2. Results and discussion

A hard pulse normal IR sequence yielded the  $T_1$  values for sodium in the saline solution and for sodium in cartilage as 64.4 and 18.2 ms, respectively, at 11.7 T. The zero-crossing points in the relaxation curves were at 39.2 ms and 12.3 ms, respectively. The zero-crossings are slightly different if low power pulses are employed (34.5 and 6.5 ms, respectively).

\* Corresponding author. Fax: +1 212 260 7905.

E-mail address: [alexej.jerschow@nyu.edu](mailto:alexej.jerschow@nyu.edu) (A. Jerschow).

A sample containing both cartilage and saline solution was imaged using a two-dimensional projection–reconstruction image (Fig. 2). By adjusting the inversion–recovery delays accordingly, one can either select the cartilage-bound sodium region, or the saline sodium in the images. In Fig. 2b, the signal of cartilage-bound sodium is essentially not reduced, largely due to the big difference in  $T_1$  values between the two sodium pools. By contrast, Fig. 2c shows, that the free sodium signal is reduced by approximately 30% due to a partial saturation at the 6.5 ms inversion–recovery delay.

The rf power was chosen to reflect the typical power attainable on MRI scanners (on the order of 500 Hz). The pulse durations (0.5 and 1 ms, respectively) are still sufficiently short such that relaxation losses during the pulses are mild [19]. The sodium  $T_1$  relaxation is biexponential [16] and the signal integral after the inversion recovery sequence is modulated by

$$f(t) = 4 \exp(-CJ_2 t) + \exp(-CJ_1 t), \quad (1)$$

where  $J_n = (2/5) \frac{\tau_c}{1+(n\omega_0\tau_c)^2}$ ,  $C = \pi^2 C_q^2 (1 + \eta^2/3)/10$ ,  $C_q$  is the quadrupolar coupling constant, and  $\eta$  the asymmetry. This biexponential relaxation mechanism will not interfere with the selection of cartilage-bound sodium, in general, since in this case, both the short and the fast components will have decayed to an appreciable extent already. In the experiment that selects the free sodium, incomplete cancellation of the bound sodium may occur, as is also seen in Fig. 2c. The ratio of the rates  $J_2/J_1$  approaches a maximum of four as  $\tau_c \rightarrow \infty$ . In general, however, one can minimize this effect by simply choosing the delay  $\tau$  of the inversion–recovery experiment to be the zero-crossing point of Eq. (1) when selecting the free sodium signal. Some contamination of the free sodium signal may occur, however, in the presence of quadrupolar coupling. While one can adjust the optimum delay  $\tau$  to compensate for such effects, a distribution of a sizable quadrupolar interaction will lead to signal contamination due to quadrupolar nutation-related effects, especially if the ratio  $\omega_{\pi}/\omega_Q$  is small [13]. Nonetheless, in the case demonstrated here, the average quadrupolar coupling was  $\omega_Q/2\pi = 370$  Hz for the cartilage tissue, and a relatively clean nulling of the cartilage-bound sodium is possible in Fig. 2c. Alternatively, one could adjust the pulse flip angles to partially compensate for nutation effects. In practice, however, it is expected that selecting the bound sodium over the free sodium signals will find more frequent use. In this case, quadrupolar nutation effects will be negligible.

In order to demonstrate this experiment *in vivo*, we calibrated the optimal free-sodium suppression condition using first an *ex vivo* bovine knee sample together with a saline bag on a 7 T scanner. Optimal suppression was found at a 40 ms inversion–recovery delay (Fig. 3a and b). In addition, since the strong signals from the saline compartment are minimized, fewer projection–reconstruction artifacts arise in the image. This aspect can be particularly important when working with undersampled data, since the sodium images become sparser. The same images were then also performed to compare the signal suppression between a regular pulsed image, and an inversion–recovery image of a human knee (Fig. 3c and d). The inversion–recovery sequence makes the demarcation of cartilage tissue more evident *in vivo*. Cross-sections showed that the signal in the cartilage region was lower by approximately 30% in the inversion–recovery sequence. A part of this reduction comes from the fact that non-cartilage compartments no longer contribute as strongly to the signals, hence the interpretability of the  $^{23}\text{Na}$  signals in terms of measuring the fixed charge density in cartilage is enhanced.

### 3. Conclusions

We present here a simple method based on inversion recovery for separating the signals from the free and cartilage-bound sodium

pools. Either pool can be selected in an image. The advantages of this method lie in (1) its simplicity, (2) its sensitivity, (3) its ability to selectively detect either the ordered or free sodium signal, (4) the relative robustness against flip angle errors, (5) its small phase cycle, (6) the detection of the central transition, and (7) its high sensitivity, which should make it more attractive than multiple-quantum filtering in  $^{23}\text{Na}$  MRI. The presented method is especially suitable for imaging cartilage. The strength of binding and the large electric field gradients that sodium experiences near the highly negatively charged proteoglycans lead to a particularly large difference of the relaxation rates between cartilage and synovial sodium.

### 4. Experimental

The experiments of Fig. 2 were carried out on a Bruker Avance 500 MHz spectrometer (11.7 T) with a BBO probe tuned to sodium frequency. The pulse sequence used is shown in Fig. 1. We optimized the relaxation delay  $\tau$  between these two pulses in order to achieve selective detection of the ordered sodium or the free sodium signal. All pulse durations were calibrated based on the free sodium signal. The rf strengths were 487 Hz for all the pulses (513.5  $\mu\text{s}$   $\pi/2$  pulse duration). 2D images were obtained from 30 1D projections using projection reconstruction. The sample consists of two capillaries of 1 mm inner diameter aligned vertically in an NMR tube. One of the tubes contains cartilage and the other a saline solution at a concentration of 55 mM by diluting a phosphate-buffered saline solution (Aldrich, pH 7.4). A gradient of 5 G/cm strength was applied in the transverse direction and 2048 data points were acquired to cover a spectral window of 10 kHz, with 64 transients coadded. The repetition delay was 1 s for all measurements. The first pulse was cycled between  $0^\circ$  and  $180^\circ$ .

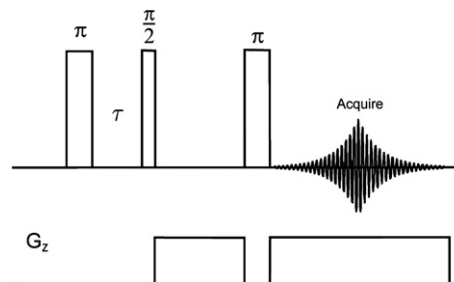


Fig. 1. Pulse sequence of the inversion recovery sequence performed in combination with a gradient spin echo.

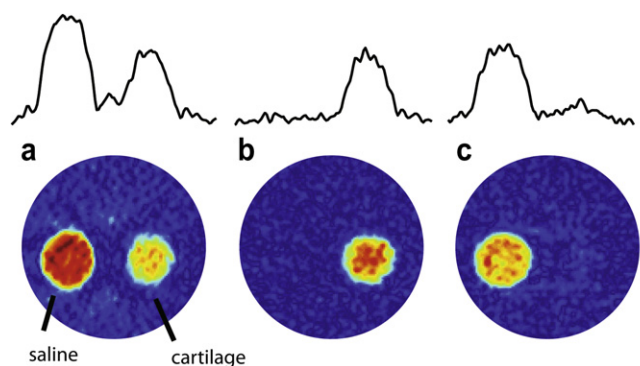
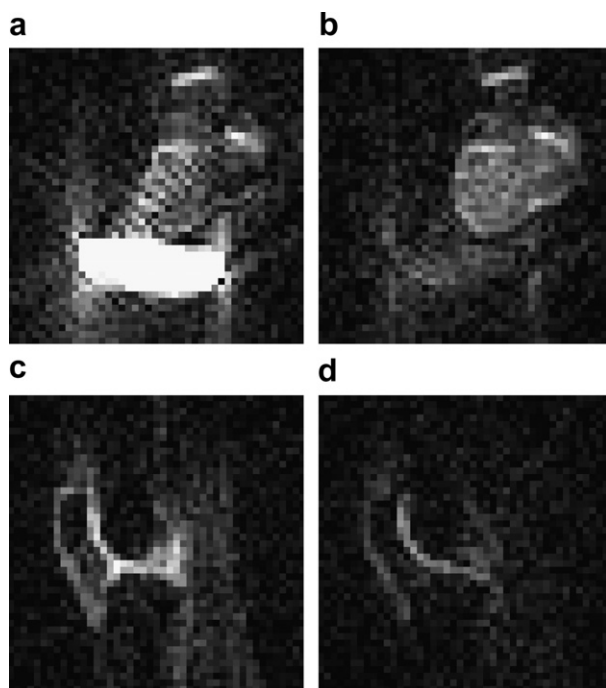


Fig. 2. 2D images obtained from 30 1D projections using projection reconstruction. The sample consists of two capillaries aligned vertically in an NMR tube. One of the tubes contains cartilage and the other a saline solution. In (a) the single-pulse response is shown, in (b) inversion–recovery with a 34.5 ms delay was used, and in (c) an inversion–recovery delay of 6.5 ms was used. 1D projections are displayed at the top to allow one to estimate the level of suppression in these experiments.



**Fig. 3.** Axial ex vivo images of a bovine knee joint with a saline bag at 7 T (a) without inversion-recovery, and (b) with an inversion-recovery delay of 40 ms. In vivo images of a human knee at 7 T (a) without inversion-recovery, and (b) with an inversion-recovery delay of 40 ms.

The experiments of Fig. 3 were performed on a 7.0 T whole body scanner with multi-nuclei capability (Siemens Medical Solutions, Erlangen, Germany). A 18 cm diameter quadrature  $^{23}\text{Na}$  knee coil was used for all the imaging measurements, and rf irradiation with 800 Hz power was used. The image was performed with a 2D FLASH-radial sequence with a spatial resolution of  $4.7\text{ mm} \times 4.7\text{ mm} \times 20\text{ mm}$ , TR/TE = 500 ms/3.2 ms, acquisition time = 1 min using a slice-selective inversion pulse of 2 ms duration. A single slice was used. The ex vivo image was performed using a bovine knee joint in axial orientation together with a 500 mL saline bag ( $155\text{ mM}[\text{Na}^+]$ ) to load the coil. The in vivo images were taken from a 42-year-old male volunteer (right knee) in sagittal orientation. A 40 ms inversion-recovery delay yielded an optimal suppression of the saline signal and was hence used for both experiments. A 2.64 ms slice selective RF inversion pulse was used in these experiments.

The bovine cartilage and knee joint samples were obtained within 5 h of animal sacrifice (4–6 months old cows) from a USDA approved slaughter house (Bierig Bros, Vineland, NJ) and then frozen at  $-20\text{ }^\circ\text{C}$  until used.

#### Acknowledgments

This work was supported by U.S. NIH Grant 1R21AR054002-01A1 and was conducted in a facility constructed with support

from Research Facilities Improvement Grant Number C06 RR-16572-01 from the NCR, NIH. NYUs NMR resources were supported by NSF Grant MRI-0116222. A.J. is a member of the New York Structural Biology Center, which is supported by the New York State Office of Science, Technology, and Academic Research and NIH Grant P41 FM66354. RRR acknowledges support from NIH grant R01-AR053133-A2.

#### References

- [1] S. Kohler, N. Kolodny, Sodium magnetic resonance imaging and chemical shift imaging, *Prog. Nucl. Magn. Reson. Spectrosc.* 24 (1992) 411–433.
- [2] E. Shapiro, A. Borthakur, A. Gougoutas, R. Reddy, Na-23 MRI accurately measures fixed charge density in articular cartilage, *Magn. Reson. Med.* 47 (2002) 284–291.
- [3] A. Borthakur, E. Shapiro, J. Beers, S. Kudchodkar, J. Kneeland, R. Reddy, Sensitivity of MRI to proteoglycan depletion in cartilage: comparison of sodium and proton MRI, *Osteoarthr. Cartilage* 8 (2000) 288–293.
- [4] A. Wheaton, A. Borthakur, G. Dodge, B. Kneeland, H. Schumacher, R. Reddy, Sodium magnetic resonance imaging of proteoglycan depletion in an in vivo model of osteoarthritis, *Acad. Radiol.* 11 (2004) 21–28.
- [5] A. Wheaton, A. Borthakur, E. Shapiro, R. Regatte, S. Akella, J. Kneeland, R. Reddy, Proteoglycan loss in human knee cartilage: quantitation with sodium MR imaging – feasibility study, *Radiology* 231 (2004) 900–905.
- [6] A. Borthakur, E. Shapiro, S. Akella, A. Gougoutas, J. Kneeland, R. Reddy, Quantifying sodium in the human wrist in vivo by using MR imaging, *Radiology* 224 (2002) 598–602.
- [7] E. Insko, D. Clayton, M. Elliott, In vivo sodium MR imaging of the intervertebral disk at 4 T, *Acad. Radiol.* 9 (2002) 800–804.
- [8] R. Reddy, E. Insko, E. Noyszewski, R. Dandora, J. Kneeland, J. Leigh, Sodium MRI of human articular cartilage in vivo, *Magn. Reson. Med.* 39 (1998) 697–701.
- [9] R. Kemp-Harper, S. Brown, C. Hughes, P. Styles, S. Wimperis,  $^{23}\text{Na}$  NMR methods for selective observation of sodium ions in ordered environments, *Prog. Nucl. Magn. Reson. Spectrosc.* 30 (1997) 157–181.
- [10] G. Navon, H. Shinar, U. Eliav, Y. Seo, Multiquantum filters and order in tissues, *NMR Biomed.* 14 (2001) 112–132.
- [11] W. Ling, A. Jerschow, Selecting ordered environments in NMR of spin-3/2 nuclei via frequency-sweep pulses, *J. Magn. Reson.* 176 (2005) 234–238.
- [12] W. Ling, A. Jerschow, Frequency-selective quadrupolar MRI contrast, *Solid-State Nucl. Magn. Reson. Spectrosc.* 29 (2006) 227–231.
- [13] A.J.J. Choy, W. Ling, Selective detection of ordered sodium signals via the central transition, *J. Magn. Reson.* 180 (2006) 105–109.
- [14] H. Shinar, G. Navon, Multinuclear NMR and microscopic MRI studies of the articular cartilage nanostructure, *NMR Biomed.* 19 (2006) 877–893.
- [15] W. Ling, R.R. Regatte, M.E. Schweitzer, A. Jerschow, The behavior of ordered sodium in enzymatically depleted cartilage tissue, *Magn. Reson. Med.* 56 (2006) 1151–1155.
- [16] G. Jaccard, S. Wimperis, G. Bodenhausen, Multiple-quantum NMR spectroscopy of  $S = 3/2$  spins in isotropic phase: a new probe for multi-exponential relaxation, *J. Chem. Phys.* 85 (1986) 6282–6293.
- [17] H. Shinar, Y. Seo, K. Ikoma, Y. Kusaka, U. Eliav, G. Navon, Mapping the fiber orientation in articular cartilage at rest and under pressure studied by 2H double quantum filtered MRI, *Magn. Reson. Med.* 48 (2002) 322–330.
- [18] K. Keinan-Adamsky, H. Shinar, G. Navon, The effect of decalcification on the microstructure of articular cartilage assessed by 2H double quantum filtered spectroscopic MRI, *MAGMA* 18 (2005) 231–237.
- [19] J.R.C. van der Maarel, W. Jesse, I. Hancu, D.E. Woessner, Dynamics of spin  $I = 3/2$  under spin-locking conditions in an ordered environment, *J. Magn. Reson.* 151 (2001) 298–313.
- [20] R. Stobbe, C. Beaulieu, In vivo sodium magnetic resonance imaging of the human brain using soft inversion recovery fluid attenuation, *Magn. Reson. Med.* 54 (2005) 1305–1310.
- [21] R.P. Kline, E.X. Wu, D.P. Petrylak, M. Szabolcs, P.O. Alderson, M.L. Weisfeldt, P. Cannon, J. Katz, Rapid in vivo monitoring of chemotherapeutic response using weighted sodium magnetic resonance imaging, *Clin. Cancer Res.* 6 (2000) 2146–2156.